Ceramics International xxx (xxxx) xxx–xxx

Contents lists available at ScienceDirect

Ceramics International

journal homepage: www.elsevier.com/locate/ceramint

Solvent free mechanochemical synthesis of MnO_2 for the efficient degradation of Rhodamine-B

Ankita Gagrani, Jingwei Zhou, Takuya Tsuzuki*

Research School of Engineering, The Australian National University, Canberra, ACT 2601, Australia

ARTICLE INFO

Keywords:
Mechanochemical processing
Manganese dioxide
Dye degradation
Photo catalyst

ABSTRACT

MnO_2 nanorods were synthesized by mechanochemical processing with subsequent heat treatment and their photocatalytic activity was studied on the decolourization of aqueous solution of Rhodamine B at different pH levels. A solid state redox reaction $2KMnO_4 + MnCl_2 \rightarrow 3MnO_2 + 2KCl + O_2$ was activated during mechanical milling. Excess KCl salt was added in the starting powder mixture to prevent agglomeration of MnO_2 nanoparticles. The milling resulted in the production of amorphous MnO_2 nanoparticles with a high surface area of 204 $m^2 g^{-1}$. Crystalline MnO_2 nanorods of diameters about 15–20 nm were produced by heating the as-milled powder at 350 °C for 1 h in air. Amorphous MnO_2 nanoparticles showed higher degradation rate of Rhodamine B than crystalline MnO_2 nanorods under simulated sunlight. The degradation rate was higher under acidic conditions. This work demonstrates the potential for cost effective, green and scalable synthesis of MnO_2 nanocatalysts for environmental applications.

1. Introduction

In recent years, organic pollutants in water have significantly increased due to intensified industrial activities. In particular, industries such as the textile, paper and cosmetic sectors release large amounts of dye effluents, which have become one of the major causes of water contamination [1]. The effluents often contain toxic and noxious dyestuffs, engendering adverse effects on aquatic life, human health and environment [2]. In the past, significant amounts of research have been conducted on developing technologies for eliminating these pollutants [3–6]. Photocatalytic reaction is one of the promising ways to remove the pollutants by utilization of sunlight, an abundant and clean energy source [7].

The photocatalytic degradation of various dyes has been investigated by using a wide variety of photocatalysts such as TiO_2 [8], ZnO [9], WO_3 [10] and bismuth compounds [6,11–13]. Among them, manganese dioxide is of significant practical interest due to its considerable redox activity, low cost and earth-abundant composition [14]. A number of efforts have been made for the development of various morphologies of MnO_2 to enhance the catalytic performance [15–17]. Yin et al. reported a simple hydrothermal synthesis of MnO_2 nanorods and studied their performance on the degradation of congo red, eosin red and methyl orange under UV-light irradiation [18]. Dang's group investigated the decolourization of methylene blue and methyl orange with a MnO_2-coated diatomite composite prepared using a wet-chemical method [19]. Combariza's group reported the removal of indigo carmine dye by a bio-nano composite produced by in situ synthesis of nanostructured MnO_2 onto natural fique fibers [20]. Fathy et al. prepared a γ-MnO_2/MWCNT nanocomposite catalyst using a co-precipitation approach and evaluated the oxidative degradation of RB19 dye [21]. Cui et al. employed refluxing process to synthesize manganese oxides with different crystal types (α-MnO_2, β-MnO_2, and δ-MnO_2) and reported decolourization of Rhodamine-B (RhB) dye at various pH levels [22].

Mechanochemical processing (MCP) is a unique bottom-up approach to synthesize a variety of nanomaterials [23–25]. It is a scalable technique utilising mechanical energy to trigger chemical reactions in a ball mill. Previously, a report by Liu et al. demonstrated the mechanochemical synthesis of MnO_2 using $KMnO_4$ and $Mn(CH_3COO)_2$ and employed H_2SO_4 to remove K^+ to study the charge-discharge properties of MnO_2 supercapacitor [26]. However, the use of H_2SO_4 during synthesis is a considerable drawback for environment. Moreover, the particle size of resulting MnO_2 was not reported. Another report by Yang et al. demonstrated the synthesis of MnO_x via a redox reaction between Mn^{7+} and Mn^{2+} in a ball mill [27]. However, the end product consisted of highly agglomerated particles.

In this work, MnO_2 nanorods were synthesized via a low cost, solvent free and scalable mechanochemical route for the first time and their photocatalytic activities to degrade dyes were investigated. A mixture of $KMnO_4$ and $MnCl_2$ was milled to initiate a solid state redox

* Corresponding author.
E-mail address: takuya.tsuzuki@anu.edu.au (T. Tsuzuki).

https://doi.org/10.1016/j.ceramint.2017.12.050
Received 20 September 2017; Received in revised form 13 November 2017; Accepted 7 December 2017

reaction $2KMnO_4 + MnCl_2 \rightarrow 3MnO_2 + 2KCl + O_2$. Excess KCl was introduced in the starting powder mixture to control the particle size of MnO_2 in the product phase. As-prepared MnO_2 showed high photodegradation efficiency towards RhB dye under the illumination of simulated sunlight at low pH. This work demonstrates a solvent free and economic fabrication method to produce MnO_2 nanoparticles with exceptional catalytic performance.

2. Experimental procedure

2.1. Preparation of MnO_2 nanoparticles

All chemicals were used without further purification. Stoichiometric amounts of $KMnO_4$ (analytical grade, Univar) and $MnCl_2$ (99.9%, Sigma Aldrich) powders were mixed in the molar ratio of 2: 1. KCl (Analar NORMAPUR, VWR) powder was added to this mixture as an inert diluent to ensure that the volume fraction of MnO_2 is 10% in the product phase in order to limit the agglomeration of MnO_2 [28]. All three chemicals were sealed in a steel vial with hardened steel balls of 9.2 mm in diameter. The ball to powder ratio of 10:1 was used for all milling operations. The mixture was milled for 4 h in a SPEX 8000 M mill (Spex, USA). The as-milled powder was heated at 350 °C for 1 h in air to crystallize amorphous MnO_2. The powder was washed thrice to remove KCl, with Millipore Milli-Q ultrapure water (18 MΩ cm) using an ultrasonic bath and a centrifuge. The remaining black powder was collected and dried in an oven at 50 °C for 9 h.

The composition of the powder was examined at room temperature using a D_2 Phaser X-ray diffraction system (XRD, Bruker, USA) with Cu-Kα radiation. The average crystallite sizes were estimated from the diffraction peak using the Scherrer equation [29]. The nanostructure and surface morphology of the powder was investigated using a CM 300 transmission electron microscope (TEM, FEI, USA) at 300 kV and a Ultra Plus field-emission scanning electron microscope (FESEM, Zeiss, Germany) at 3 kV. The specific surface area of nanopowders was measured by the Brunauer-Emmett-Teller (BET) N_2-gas adsorption method using a TriStar 3020 (Micromeritics, USA). Prior to BET measurements, the powders were degassed at 150 °C for 24 h. UV–vis absorption spectra were collected using a Varian Cary 60 spectrometer (Agilent, USA). Optical band gap energies were estimated by converting UV–vis absorption spectra into Tauc plots [30].

2.2. Photocatalytic degradation of Rhodamine B

Photocatalytic degradation of RhB dye was studied to evaluate the photocatalytic activity of MnO_2 samples. A small amount of MnO_2 (8 mg) was dispersed in 50 ml of an aqueous RhB solution with a concentration of 0.0096 mg ml^{-1}. The pH of the solution was adjusted with HCl. A low-density polyethylene film (> 85% transparent to UVA and UVB) was tightly wrapped to seal the mouth of the silica beaker for preventing the evaporation of water. Subsequently, the suspension was irradiated with simulated sunlight using a Suntest CPS+ instrument (Atlas, USA) equipped with a 1500 W xenon lamp and a daylight reduced IR filter. The irradiation intensity was 65 W m^{-2} over the wavelength range of 300–800 nm. The aliquots (4 ml) were collected at various irradiation times and immediately centrifuged at 12,000 rpm for 10 min to remove catalyst nanoparticles from the RhB solution. The Optical absorption of the RhB solution was measured using a Cary 60 spectrophotometer (Agilent, USA) to observe the photocatalytic degradation of RhB. The degradation of RhB was also investigated without light irradiation otherwise under the same conditions for both amorphous and crystalline samples.

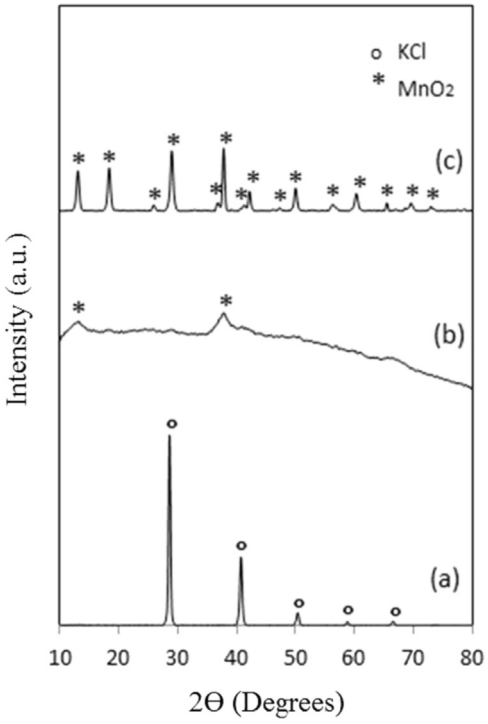

Fig. 1. XRD patterns of (a) as-milled powder milled for 4 h, (b) after subsequent washing and drying, and (c) powder milled for 4 h followed by heat treatment at 350 °C, washing and drying.

3. Result and discussions

3.1. MnO_2 nanoparticles

Fig. 1(a) shows the XRD pattern of the powder milled for 4 h. The pattern predominantly consists of peaks corresponding to KCl (JCPDS card no. 73-0380) due to the presence of excess KCl in the powder mixture. Fig. 1(b) represents the XRD pattern of the powder after washing to remove KCl. The lack of well-defined sharp peaks, except two broad peaks near 13° and 37°, can be attributed to the amorphous-like nature of the powder. Fig. 1(c) represents the XRD pattern of the powder after heat treatment at 350 °C for 1 h in air and subsequently washed, where the diffraction peaks can be indexed to α-MnO_2 (JCPDS card no. 72-1982).

Fig. 2(a) and (c) show a typical SEM and TEM images of MnO_2 samples without heat treatment. The sample consisted of irregular-shaped particles and few needle-like structures of less than 10 nm in diameter. The inset in Fig. 2(c) is a selected area electron diffraction pattern, showing rings with only few spots. The result indicates poor crystalline nature of the MnO_2, consistent with the XRD data (Fig. 1b). The few spots on the diffraction rings may stem from the needle-like structure visible in the SEM image. The needle-like structure was not observed in TEM images, possibly due to the scarcity of the structure. Fig. 2(b) and (d) show the respective SEM and TEM images of crystalline MnO_2 that was obtained after heat treatment. The sample consisted of only nanorods of about 15–20 nm in diameter with varying lengths. The inset in Fig. 2(d) shows lattice fringes running parallel to the surface of a nanorod along the length direction. The lattice spacing between adjacent planes was ~ 0.7 nm corresponding with the distance between two (110) crystal planes of α-MnO_2. The average crystallite size estimated using the diffraction peak corresponding to (110) crystal plane at 13° was 16 nm. This value is in good agreement with the observed diameter of nanorods. The BET surface areas of the amorphous and crystalline MnO_2 powders were 204 $m^2 g^{-1}$ and 76 $m^2 g^{-1}$, respectively.